Published in final edited form as:
Arch Biochem Biophys. 2010 January 15; 493(2): 184–191. doi:10.1016/j.abb.2009.10.014.

Spectroscopic studies of the oxidation of ferric CYP153A6 by peracids: Insights into P450 higher oxidation states

Tatyana Spolitak[a], **Enrico G. Funhoff**[b,c], and **David P. Ballou**[a,*]

[a]Department of Biological Chemistry, Medical School, University of Michigan, Ann Arbor, MI 48109-5606, USA [b]Swiss Federal Institute of Technology, CH-8093 Zűrich, Switzerland

Abstract

Our previous rapid-scanning stopped-flow studies of the reaction of substrate-free cytochrome P450cam with peracids [T. Spolitak, J.H. Dawson, D.P. Ballou (2005) J. Biol. Chem. 280, 20300-20309; (2006) J. Inorg. Biochem. 100, 2034-2044; (2008) J. Biol. Inorg.Chem. 13, 599-611] spectrally characterized compound I (ferryl iron plus a porphyrin π-cation radical (Fe^{IV}=O/Por $^{\bullet+}$)), Cpd ES, and Cpd II (Fe^{IV}=O/Tyr$^{\bullet}$ or Fe^{IV}=O). We now report that reactions of CYP153A6 with peracids yield all these intermediates, with kinetic profiles allowing better resolution of all forms at pH 8.0 compared to similar reactions with WT P450cam. Properties of the reactions of these higher oxidation state intermediates were determined in double mixing experiments in which intermediates are pre-formed and ascorbate is then added. Reactions of heptane-bound CYP153A6 (pH 7.4) with *m*CPBA resulted in conversion of P450 to the low-spin ferric form, presumably as heptanol was formed, suggesting that CYP 153A6 is a potential biocatalyst that can use peracids with no added NAD(P)H or reducing systems for bioremediation and other industrial applications.

Keywords

Cyp153A6; peracids; Cpd I; Cpd II; alkane hydroxylation; cytochrome P450; ferryl intermediates

INTRODUCTION

Cytochrome P450 enzymes (CYP) are involved in the biodegradation of many hydrophobic compounds, including a wide variety of endogenous and exogenous organic chemicals [1;2]. CYP enzymes typically oxygenate such compounds to form alcohol products. One of the primary goals in cytochrome P450 research is to characterize reactive intermediates that might be involved in these P450-catalyzed oxygenation reactions [3-7]. Evidence that multiple oxidizing species of P450 may be involved in the various types of reactions that includes a diversity of its substrates makes characterization of active transients a subject of intense investigation [1;3;5;8-11]. Cpd I is thought to be the primary oxygenating species in most P450 reactions, and in vivo it evolves by a complex series of reactions involving the reduction of the ferric P450 followed by reaction with oxygen to form an oxyferrous species, addition of a

*To whom correspondence should be addressed: David P. Ballou, phone: 1-734-764-9582 , fax: 1-734-763-4581, dballou@umich.edu.
[c]Current address: Novartis Institutes for Biomedical Research Investigative Toxicology, Basel, Switzerland

second electron, and subsequently, a proton to form a nascent peroxo-complex. This complex undergoes heterolytic cleavage to form H_2O and Cpd I ($FeIV{=}OPor^{\bullet+}$), considered to consist of a ferryl (oxo-iron) coupled to a π-cation radical of the porphyrin [1;3;10-15]. Cpd I is oxidized by two electrons with respect to the ferric state. In normal catalysis the electrons are delivered by reductases consisting of flavoproteins and iron-sulfur proteins that are specific for each P450 system. One of the important approaches for studying hydroxylation mechanisms of P450 and its active intermediates employs peracids, alkylhydroperoxides, or H_2O_2 to provide both the oxygen and the reducing equivalents to P450 simultaneously. This process, referred to as the shunt pathway, permits the study of P450 intermediates in the absence of a reductase system, thus simplifying the reaction and eliminating requirements for anaerobic conditions and additional components. The disadvantage of the shunt pathway is that it usually leads to eventual heme destruction, so that it is difficult to fully characterize many of the intermediates.

Previously, we showed that in the absence of camphor, reactions of P450cam with *m*CPBA as oxidant generated an intermediate that was spectroscopically characterized as Cpd I, with an absorbance maximum at ~370 nm, as well as a species referred to as Cpd ES, with an absorbance maximum at ~407 nm [14;15]. Cpd ES, which is oxidized by two equivalents with respect to ferric P450, arises by intramolecular electron transfer from nearby tyrosines or tryptophans that reduces the porphyrin π-cation radicals of Cpd I. Cpd ES, produced by reaction of substrate-free P450cam with peracetic acid, has been characterized by rapid freeze-quench Mössbauer and EPR spectroscopy to be a form of Cpd II plus a tyrosyl radical [16-18]. The tyrosine radicals were assigned to Tyr96 for wild type P450cam, and to Tyr 75 for the Tyr96Phe variant [16]. These tyrosines are within 7 Å of the heme. By using manual freeze-quench-EPR techniques on the reaction of $P450BM_3$ with *m*CPBA as oxidant at pH 6.8, Raner et al [19] provided evidence that the appearance of the protein radical of Cpd ES correlated with the development of the 407 nm Soret band.

Our studies on P450cam showed that Cpd ES can form, although more slowly, even if the nearby tyrosines are replaced by phenylalanines in Tyr75Phe/Tyr96Phe P450cam variant [15]. suggesting that in the absence of a suitable (hydroxylatable) substrate, Cpd I will eventually convert to a less reactive Cpd ES species by oxidizing more distant tyrosines or tryptophans. If Cpd ES were to form in the presence of NAD(P)H and the reductase components, one electron would be delivered rapidly to reduce Cpd ES to Cpd II, and a second electron would be added to regenerate ferric P450 and H_2O. Thus, with complete P450 systems, when a suitable substrate is not present and Cpd I forms, the overall reaction constitutes an NAD(P)H peroxidase mechanism that defuses the strongly oxidizing Cpd I without releasing any reactive oxygen species [15].

The reactions of P450cam described above have precedence in peroxidases, where the porphyrin π-cation radical of Cpd I is normally reduced by one electron that is delivered from reducing substrates to form Cpd II, and then by another to return the heme to the ferric state. Cpd II, which can be represented as $Fe^{IV}{=}O$ (or Fe^{IV}-OH in its protonated form), is oxidized by one electron with respect to the ferric state. Cpd II of P450 in its unprotonated form is often characterized by a Soret band at ~420 nm.

In our previous studies with site-directed mutant forms of P450cam [20] we showed how changes in hydrogen bonding patterns and increased hydrophobicity of the heme active site influence the formation of Cpd II in reactions with peracids and with cumene hydroperoxide. The reaction of P450cam with organic peroxides or peracids initially forms peroxo- or acylperoxo- heme intermediates that can split either heterolytically to form Cpd I plus an alcohol or acid (as described above), or homolytically to form Cpd II and a neutral organic hydroxyl or acid radical. The first step resulting in the formation of the acylperoxo-iron(III)

porphyrin intermediate has been demonstrated with models and with heme proteins to be an intermediate in the formation of Cpd I [21-28].

Both the heme environment and the pH can affect the relative fractions of acylperoxo-complex that undergo homolysis and heterolysis. More hydrophobic environments and higher pH favor homolytic breakdown of the peroxo-P450 to produce neutral products, rather than heterolytic cleavage that would result in acid, alkoxyl, or hydroxyl leaving groups. We showed that under some conditions, in addition to forming via homolysis, Cpd II can also accumulate by reduction of Cpd I, analogously to its formation in peroxidase cycles [20]. The Cpd II-like species, however, was found to be ineffective in hydroxylating camphor, although it could be readily reduced to ferric P450cam by ascorbate or other reductants. The resultant ferric form of P450cam was verified by its ability to bind camphor, which is easily recognized by its high spin heme spectrum with its Soret band at ~392 nm [20]. In fact, addition of reducing agents to either of the high-valent species (Cpd ES or Cpd II) reforms the Fe^{III} state and prevents most of the destruction of the heme that normally occurs in extended reactions with peroxides and peracids. Although Cpd ES and Cpd II both have a Fe^{IV}=O (ferryl) chromophore, Cpd ES (characterized by a Soret band at ~407 nm) was most readily seen at lower pH, while Cpd II (Soret band at ~420 nm) was observed at pH $\geq$ 7.5. When Cpd II that was formed at pH 8.0 was mixed with buffer to change the pH to 6.20, the Soret band rapidly shifted to 407 nm, which is consistent with this idea. We suggested that the species having a Soret absorption peak at ~420 nm was the unprotonated form of Cpd II while that absorbing maximally at 407 nm (Cpd ES) was the protonated ferryl [20].

In the work reported here we have focused on kinetic studies of CYP153A6 from *Mycobacterium* sp. HXN-1500 and compared the results to those for P450cam and BM3. P450cam, $P450BM_3$, P450cin, P450biol, the thermophylic CYP119 [29-31], and several strains of the CYP153 family of enzymes have been shown to hydroxylate linear alkanes and fatty acids at the terminal position [32]. The P450 enzymes from the CYP153 family, which have been found in cells growing on *n*-alkanes [33], appear to occur as soluble proteins [34], like many other bacterial P450s. Most bacterial P450s accept electrons either from flavoproteins containing both FAD and FMN, or from ferredoxins (FD) that are reduced by flavoprotein ferredoxin reductases (FDR). CYP153 enzymes require the presence of both FD and FDR. Eight different CYP153 genes have been functionally expressed in *Pseudomonas putida*, which is able to use aliphatic alkanes ranging from pentane to dodecane as sole carbon and energy sources [32;35]

CYP153A6 from *Mycobacterium* sp. HXN-1500 hydroxylates medium-chain alkanes (C_6 to C_{11}) to 1-alkanols with regio-specificities of $\geq$ 95 % for the terminal carbon atom position [32]. CYP153A6 has been shown to be useful for biocatalytically producing valuable biochemicals, including pharmaceuticals from hydrophobic compounds. For example, *Sphingomonas* sp. HXN-200, which harbors one CYP153, was reported to be able to hydroxylate piperidines, pyrrolidines, and azetidines to use for producing pharmaceutically valuable compounds [36;37]. The broad substrate spectrum and the ability to carry out terminal alkane hydroxylations make the CYP153 and related P450 enzymes especially promising for biocatalytic syntheses of useful chemicals. Other cytochrome P450s, such as P450cam and $P450BM_3$, can also be modified by site-directed mutagenesis to enhance their binding propensities and reactivities toward smaller substrates and to increase their robustness during biocatalytic synthesis of products. In addition, the active sites of P450 enzymes have been engineered to optimize the oxidation of non-natural substrates [38].

In this work we have used artificial oxygen donors to investigate intermediates involved in the reactions of the CYP153A6. As predicted from our previous studies, the more hydrophobic active site of CYP153A6 allows accumulation of Cpd II rather than Cpd ES species in reactions

with peracids. Cpd I, Cpd ES, and Cpd II (at higher pH) could all be observed with CYP153A6 under a variety of conditions due to the unique nature of the CYP153A6 active site compared to that of P450cam and BM_3. These studies help to define characteristics that facilitate hydroxylation of unreactive alkanes (with high regio-selectivity at terminal positions). We have compared the kinetics and other characteristics with those for similar reactions with P450cam and $P450BM_3$ and have shown the effects of adding external reductants such as ascorbate at various pH values. We demonstrate that substrate-bound CYP153A6 can yield oxygenated products using the shunt pathway. These results help the understanding of how artificial oxidants can be used with CYP153A6 for biotechnological applications.

MATERIALS AND METHODS

P. putida containing an expression vector (pCom8) with a polycistronic construct of the CYP153A6 P450, ferredoxin, and ferredoxin reductase from *Mycobacterium* sp. HXN-1500 has been described [37]. P450 CYP153A6 was isolated without the ferredoxin and ferredoxin reductase, as previously described [32], and stored in 50 mM phosphate buffer, pH 7.4, containing 5% glycerol. Before use, it was equilibrated with 50 mM potassium phosphate buffer at desired pH, by passing it through a G–25 column. All reagents were obtained from commercial sources. Spectrophotometric measurements were performed with a Shimadzu UV-2501PC UV-visible absorption spectrophotometer. The peracids were standardized spectrophotometrically using the triiodide assay ($\varepsilon_{353\ nm}$ = 25.5 mM^{-1} cm^{-1}) [39]. All kinetic experiments were performed at either 4 or 25 °C, and at pH 6.2, 7.4, and 8.0 in 50 mM phosphate buffer containing 100 mM KCl. Freshly prepared enzyme and peroxidase substrates were used for all experiments.

Kinetic data were acquired using a Hi-Tech Scientific, Ltd Model SF-61 stopped-flow spectrophotometer. The dead time was determined to be 1.5 ms. For diode array assays the Hi-Tech SF-61 DX-2 was used with a 1.5 ms integration time. Concentrations given in figure legends are those after mixing the reactants, unless otherwise specified. Stock solutions of heptane in DMSO were prepared so that the concentration of DMSO used for stopped-flow experiments was ~0.5% by volume. Data collection and analysis were performed using program A based on the Marquardt-Levenberg algorithm [40] and developed in our laboratory by R. Chang, C-J. Chiu, J. Dinverno, and Dr. D.P. Ballou, by KinetAsyst 3 (High-Tech Scientific), and by the Specfit Global Analysis Program (Spectrum Software Associates). Singular value decomposition of data was performed using the Specfit Global Analysis Program. The fitting to models described below treated the first step as a pseudo-first order reaction due to the presence of excess of peracid.

The product analysis was done by GC/MS as described [32], using ethyl acetate and methylene chloride for extraction, and the samples were concentrated under argon to a final volume of 100 μL. A Thermo-Finnigan Trace MS system was used. Separation was achieved on a Supelco SLB-5MS (30 m × 0.25 mm i.d. film thickness) column. Splitless injections were made into an injector maintained at 200 °C.

RESULTS

Reactions of CYP153A6 with peracids at pH 8.0, 25 °C

CYP153A6 has a rather hydrophobic site that is suitable for binding unreactive alkanes as substrates. Therefore, it was expected on the basis of our earlier studies on the more hydrophobic tyrosine variants of P450cam described above that CYP153A6 would be likely to form substantial quantities of Cpd II. We have carried out our experiments at higher pH values, reasoning that such conditions would also favor formation of the putative Cpd II for this enzyme. Fig. 1A shows spectra recorded during the reaction of CYP153A6 with excess

*m*CPBA. The spectrum of the ferric low spin form (the starting P450) before mixing is presented for reference. The trace recorded at 367 nm (Fig. 1A, inset) shows an increase of absorbance in the first 21 ms that is largely attributed to the formation of some Cpd I. The traces at 417 and 408 nm show that at least two steps follow the formation of the putative Cpd I.

SVD and global fitting analysis of the data, using the model A → B → C → D, with k_1 = 91 s^{-1}, k_2 = 22.5 s^{-1}, k_3 = 1.5 s^{-1} yielded the spectra shown in Fig. 1B; spectrum A is that of the ferric substrate-free CYP153A6, and spectrum B has characteristics of a mixture of an acylperoxo-complex and Cpd I. The peak at 367 nm is attributed to Cpd I, and it is similar to the Soret for Cpd I of *Caldariomyces fumago* chloroperoxidase (CPO) [41], which also has a broad Soret peak at 367 nm as well as broad weak band at ~ 695 nm. CPO Cpd I has been shown to consist of an exchange-coupled S=1 Fe^{IV}=O and a spin S = ½ porphyrin [42]. The results with CYP153A6 in Fig. 1 suggest that the initial formation of the acylperoxo-complex and its subsequent conversion to Cpd I are not kinetically well separated; therefore, they appear in a single phase with an apparent rate constant of 91 s^{-1}, resulting in species B. Global fitting of the data led to the conclusion that the mixture of the acylperoxo-complex and Cpd I accumulated to ~65% of the total enzyme by ~25 ms (Fig. 1C).

The second phase (22.5 s^{-1}) results in the calculated spectrum C with a Soret band near 421 nm, this is attributed largely to Cpd II (the analysis in Fig. 1C suggests that ~80% of the enzyme exists as the ~421 nm species at 150 ms). This phase is indicated by the increase in absorbance at ~417 nm (Fig. 1B), a prominent β-band at ~536 nm, and an α-band at ~570 nm (see inset, Fig. 1B). The spectral changes are similar to those observed for P450cam Tyr-to-Phe variants in the reaction with *m*CPBA at pH 8.0. This process is followed by a slower phase over the next 160 ms that results in formation of species D, with an absorbance maximum at ~408 nm. The spectrum of D appears to be due to a mixture of bleached heme and Cpd ES, formed as a result of intramolecular electron transfer to Cpd I [43]. By contrast, very little Cpd ES was detected for Tyr variants of P450cam at pH 8.0; instead, formation of Cpd I was followed by partial formation of Cpd II (Soret ~420 nm), as well as considerable bleaching of the heme [14;20]. Thus, with Cyp153A6, both homolytic and heterolytic processes appear to be involved, and all of the known higher oxidation state intermediates can be partially resolved at pH 8.0.

We also carried out reactions under the same conditions using deuterated buffers in an attempt to better resolve steps involving protons. We reasoned that deuterated solvents would be more likely to affect the formation of Cpd ES (which consists of the protonated form of Cpd II plus an aromatic radical) and help us to resolve intermediates more clearly. We carried out the reaction at 25 °C, pD 8.4. However, the results were nearly the same, including the resolution of the same intermediates, as in the presence of H_2O. Rate constants obtained were: k_1= 88 s^{-1}, k_2 = 18 s^{-1}, k_3 = 1.3 s^{-1}.

Fig. 2 shows the reaction at 3.4 °C; the spectral changes are similar but slower than those observed at 25 °C (time courses for various wavelengths are shown in the inset of Fig. 2A). SVD and global analysis of the diode array data (at the rates 34 s^{-1}, 3s^{-1}, 1.4 s^{-1}) resolved the formation of a spectrum of B at 34 s^{-1} (mixture of acyl-peroxocomplex and some of Cpd I), species C (Cpd II, 2.8 s^{-1}) with an absorbance max at ~420 nm that preceded formation of Cpd ES (Soret peak at ~407 nm). The rate for the formation of Cpd I was 2.6 –fold slower, and the rate for formation of the Cpd II-like species was 7.5-fold slower than those observed under the same conditions at 25 °C.

Reaction of CYP153A6 with mCPBA at pH 7.4 and 6.2

The spectral changes in the reaction of *m*CPBA with substrate-free ferric CYP153 at lower pH are qualitatively similar to those reported previously for P450cam[14;15], except that all of the

processes are slower for CYP153A6. Fig. 3A shows spectra recorded during the first 0.6 s of the reaction with *m*CPBA at pH 7.4. The increase in absorbance at 367 nm (first 19 ms, inset Fig. 3A) leads to a spectrum with a Soret band at ~420 nm with low intensity that appears to be a mixture of the acyl-peroxocomplex and some Cpd I species (absorbance at ~365 nm). Over the next ~150 ms this mixture converts at 13.5 s^{-1} to a species with an absorbance maximum at 407 nm. SVD and global kinetic analysis of the data using an A → B → C → D model with k_1 = 120 s^{-1}, k_2 = 13.5 s^{-1}, k_3 = 1.9 s^{-1} (Fig. 3B) reveals characteristic spectra of the relevant species. Spectrum A is of the starting CYP153, spectrum B is due to a mixture of the acyl-peroxo and Cpd I species, indicated by the increase in absorbance at both ~367 and at ~695 nm, and spectrum C is clearly resolved with an absorbance maximum at 407 nm; it is essentially indistinguishable from the Cpd ES species reported previously for both P450cam [14;15] and P450 BM3 at pH 6.2 [19]. Spectrum D is due to an undefined mixture of species that includes bleached heme. The rate of formation of Cpd ES (13.5 s^{-1}) compared to its decay (~1.9 s^{-1}) results in the accumulation of >75% of the P450 as Cpd ES, and this is considerably more than observed at pH 8. This spectrum of Cpd ES has a Soret band at ~407 nm, and the ferryl is likely to be protonated.

The spectral changes observed during the reaction of CYP153 at pH 6.2, 25 °C (8.8 μM of P450, 19 mM *m*CPBA) are shown in Fig. 4A. Very little (if any) Cpd I can be discerned (first 20 ms). After a brief lag (~20 ms) during which the absorbance at 419 nm decreases slightly, Cpd ES forms at 12.5 s^{-1}, which is very similar to that seen at pH 7.4. The spectral changes are similar to those observed with P450cam. SVD and global analysis of the data using the model A → B → C with k_1 = 85 s^{-1}, k_2 = 12.5 s^{-1} reveals a spectrum B that may be a mixture of the acyl-peroxocomplex and a small amount of Cpd I (forming at 85 s^{-1}), and spectrum C (forming at 12.5 s^{-1}) that clearly corresponds to a Cpd ES species. Nearly all of the CYP153A6 seems to accumulate as Cpd ES, and this species is stable for more than one second. As with P450cam, the reactions of CYP153A6 with peracetic acid (2.4 mM) to form Cpd ES were slower than those with *m*CPBA

Reactivities of intermediates

In our previous double-mixing stopped-flow studies, we showed that addition (in the second mix) of reductants such as guaiacol, ferrocyanide, ascorbate, or TMPD would reduce to the ferric state any of the various ferryl species, including these of Cpd I, Cpd ES, and Cpd II that had been formed in reactions of either P450cam or P450 BM3 with *m*CPBA. The addition of these reductants also prevented most of the bleaching of the heme that was always observed in their absence. These observations are consistent with peroxidase chemistry being carried out by P450, and imply that ferryl species are formed during reactions of P450 with *m*CPBA. We have performed double-mixing stopped-flow studies to first produce various ferryl species and then to reduce the ferryl species with reductants such as guaiacol, ferrocyanide, ascorbate, or TMPD. Fig. 5 shows the spectral changes that occurred at pH 8, 25 °C after CYP153A6 was first mixed with *m*CPBA for 36 ms and then reacted with guaiacol in the second mix. Cpd I and Cpd II (~50% each - see Fig. 1) that had been maximally formed by 36 ms, reacted with guaiacol to form the colored product, oxidized guaiacol (see Fig. 5). The trace recorded at 470 nm (Fig 5, inset) shows an increase of absorbance occurring at ~1.73 s^{-1} that is due to the oxidation of guaiacol (The observed oxidation of guaiacol in this figure is due to several complete turnovers of CYP153A6. The trace at 470 nm in the inset to Fig. 5 indicates that by ~3 s the *m*CPBA has been consumed. Given that the *m*CPBA : CYP153A6 ratio was 20, the overall turnover number can be estimated to be ~7 s^{-1}). This rate is slower than those for Cpd ES forms of P450cam WT and its Tyr variants (at least, 3.5-fold slower). Note that under these conditions the oxidized guaiacol product is not stable, as indicated by the decrease of absorbance at 470 nm at times > 3 seconds.

We also carried out experiments with CYP153A6 to examine the pH-dependence of how the higher oxidation states of CYP153A6 are reduced by ascorbate. In double mixing experiments CYP153A6 was first mixed with *m*CPBA, and then in the second mix with ascorbate at various pH values. The aging time before the second mix was chosen to produce a mixture of ~50% each of Cpd I and Cpd II before reacting with ascorbate (38 ms at pH 8.0, 25 °C, Fig. 6). Addition of ascorbate in the second mix resulted in a fast phase at ~160 s^{-1} and a second phase at ~12 s^{-1}. The faster phase for CYP153A6 (163 s^{-1}) (Fig.7) is attributed to the reaction of ascorbate with Cpd I, whereas the slower phase was attributed to the reduction of Cpd II to the ferric form. This difference in rates of reduction of Cpd I and Cpd II is similar to that often seen for peroxidases.

Some interesting characteristics were found at pH 7.4, 25 °C. In double-mixing experiments, addition of ascorbate to the reaction mixture of CYP153A6 and *m*CPBA after an aging time of 55 ms did not prevent the initial accumulation of Cpd ES (Fig. 7); Cpd ES continued to be formed after addition of ascorbate and then was slowly reduced to the ferric form over a period of ~10 s. This result suggests that formation of Cpd ES (i.e., Cpd I → Cpd ES) is faster than ascorbate binds and reduces Cpd I to the ferric form. One of the reasons for the slower reaction of CYP153A6 with ascorbate compared to that for P450cam might be due to weaker binding of ascorbate to the protein in the more hydrophobic environment of CYP153A6 active site. Consistent with this notion, the reactions of Cpd ES and Cpd II species of the Y96F and Y96F/Y75F P450cam variants with ascorbate were also slower than with wild type, probably due to the increased hydrophobicity of the heme pocket of these variants [15;20]. Interestingly, either NADH or NADPH (~620 μM) could reduce Cpd ES slowly (9.26 s^{-1}; 0.85 s^{-1}) in a reaction very similar to that with ascorbate (8.5 s^{-1}; 0.91 s^{-1}). Because there was no ferredoxin or its reductase present, this reaction must have occurred via direct reduction of Cpd ES. Addition of ABTS in the second mix to the initially preformed Cpd ES of CYP153A6 (pH 7.4, 25 °C) also resulted in reducing it to the ferric state (data not shown).

Reaction of CYP153A6 with heptane

We examined whether heptane-bound CYP153A6 could react with *m*CPBA. Our earlier studies showed that addition of *m*CPBA to camphor-bound P450cam did not produce any observable spectral changes unless a large excess of *m*CPBA was added. This lack of reactivity was attributed to camphor restricting access to the active site. The binding of heptane to CYP153A6 can be detected spectrally by its causing a shift from partially low spin to nearly fully high-spin form, analogously to that observed for the binding of camphor to P450cam [44;45]. The K_d value for CYP153A6 binding to heptane was determined to be ~0.48 μM) [32], similar to those for P450cam with camphor [46]. Double mixing experiments (pH 7.4) in which heptane was first mixed with CYP153A6 and aged for 100 s, and then reacted with *m*CPBA in the second mix, show conversion from a high-spin to a low spin ferric state within ~ 1 s (Fig. 8), indicating that *m*CPBA has at least some access to the heptane-bound ferric CYP153A6. The kinetic data recorded at 392 and 418 nm that are shown in the inset to Fig. 8 can be described by two phases of ~100 s^{-1} and 6.2 s^{-1}. The first small phase could be due to the formation of some acylperoxo-complex and Cpd I (Fig. 8). The second larger phase characterized by an increase in absorbance at 418 nm (at 6.2 s^{-1}) that leads to formation of low spin ferric P450 might be attributed to the release of the product (heptanol). We were able to detect small amounts of heptanol in the eluent from the stopped-flow instrument. The solubility of heptane is only ~24 μM [32], which limits concentration of heptanol produced, even with multiple turnovers, Because the extraction and analysis procedure is complicated, 24 μM heptanol was at the limitations of our detection capability, and this prevented quantification.

We repeated the above experiment using *m*-chlorobenzoic acid instead of *m*CPBA to ascertain whether the conversion of the heptane-bound CYP153A6 intermediate to the low spin ferric

form (Fig. 8) could be due simply to the displacement of the heptane by *m*CPBA rather than to a chemical reaction. No changes were observed upon adding the m-chlorobenzoic acid, strongly suggesting that the formation of the low spin ferric complex seen in Fig. 8 was due to a chemical reaction, not simply to displacement of the heptane.

Discussion

The reaction of CYP153A6 with artificial oxidants is characterized by spectral changes similar to those observed for substrate-free ferric P450cam WT, its Tyr-to-Phe variants, and cytochrome P450BM$_3$ *from Bacillus megaterium*. These P450s each exhibit distinct kinetic profiles that are dependent on pH. At pH 8 the reaction of *m*CPBA with WT P450cam yields a considerable fraction of Cpd I, but very little Cpd ES or Cpd II [14]. With the Tyr distal mutants (Y96F and Y75F), which have more hydrophobic active sites than WT P450cam, very little Cpd I or Cpd ES can be discerned, but >50% of the P450 accumulated as Cpd II before heme bleaching occurred. In contrast, the reaction of *m*CPBA with CYP153A6 at pH 8 (Figs. 1,2) yields a mixture of Cpd I (~367 nm) and the acylperoxo complex (apparently in a single phase at ~90 s^{-1}), and subsequently, a considerable amount of Cpd II forms in the second phase (species C in Fig. 1B). The second phase is attributed to the formation of Cpd II (unprotonated form) on the basis of the primary Soret band being at ~420 nm and there being a prominent peak at ~535 nm (Fig 1B, inset), as described earlier [20]. Cpd II appears to convert in a slower third phase to a mixture of Cpd ES and bleached heme (species D in Fig. 1B). A similar oxidation of Cpd II to Cpd ES has been demonstrated with myoglobin [47]. Because Cpd ES is less oxidizing than Cpd I, once it has formed, it is not as likely as Cpd I to be reduced by *m*CPBA to Cpd II. Moreover, these observations suggest that any highly oxidizing Cpd I that did form at this higher pH was reduced by the peracid to Cpd II faster than its conversion to Cpd ES by intramolecular electron transfer [15].

Cpd II has been an elusive species to characterize in P450cam WT, except its special form as Cpd ES or when a mild reducing agent such as methanol is present [15-17;20]. We have recently been able to detect it in P450cam Tyr-to-Phe distal variants [20] and now in WT CYP153A6 (pH 8.0). All of these enzymes have more hydrophobic heme pockets than WTP450cam. We suggest that these more hydrophobic environments tend to promote the stabilization of Cpd II.

At low pH (6.2) Cpd ES (in its protonated state) is formed during the reaction of CYP153A6 with *m*CPBA in nearly 100% yield by ~1 s. The first observed step has only small spectral changes and is likely to be primarily due to the binding of the peracid and the formation of the acylperoxo complex. Only a small amount of Cpd I accumulates, because as soon as it forms, it converts to Cpd ES via intramolecular electron transfer (probably coupled with proton transfer) from nearby oxidizable residues (e.g., Trp or Tyr) to the porphyrin π-cation radical of Cpd I. The formation of nearly stoichiometric quantities of Cpd ES at pH 6.2 was also seen with P450cam WT and its Y75F, Y96F, and Y96F/Y75F variants [14;15]. However, the rates of formation of Cpd ES with WT P450cam and its single mutants were ~4-fold greater than with CYP153A6; the rates with the latter were more similar to that with the double mutant (Y96F/Y75F) of P450cam, which had both nearby tyrosines replaced with less oxidizable phenylalanines. Consistent with the formation of Cpd ES in CYP153A6 being slower than with P450cam, Funhoff et al. [32] have indicated by homology modeling that there are no tyrosines or tryptophans in the immediate vicinity of the heme in CYP153A6. Thus, in CYP153A6 the electron that reduces the π-cation porphyrin radical must derive from a more distant aromatic residue, analogously to the Y96F/Y75F variant of P450cam. For any given concentration, the reaction of peracetic acid with CYP153A6 at pH 6.2 is about 9-fold slower than that with *m*CPBA. Thus, less Cpd ES accumulates in the reactions with peracetic acid than with mCPBA because of competition with subsequent processes such as bleaching (data not shown).

Even at pH 7.4 and pH 8.0, Cpd ES can be clearly observed with CYP153A6 in its reactions with *m*CPBA. At pH 7.4 ~75% of the P450 accumulated as Cpd ES by 160 ms, as judged from comparing the actual data (Fig. 3A) to the spectrum derived from the multi-component analysis (Fig. 3B).

For P450cam, both the 406 (Cpd ES) or the 420 nm (Cpd II) species (generated in the reaction with cumene hydroperoxide or with peracids at higher pH [20]) were shown in double mixing experiments to be readily converted back to ferric by external reductants such as ascorbate, guaiacol, ferrocyanide, or TMPD. However, with CYP153A6 at pH 7.4, Cpd ES continues to form even after ascorbate is added (Fig. 7). This result suggests that the intramolecular electron transfer to form Cpd ES is faster than the reaction of Cpd I with ascorbate. The ferric form is not fully formed until after 10 s. In contrast to these results, at pH 8, the reaction of *m*CPBA with CYP153A6 shows very little formation of the species with a Soret at 407 nm (Cpd ES) by 38 ms after reaction with mCPBA (Fig 1). In double mixing experiments at pH 8 when ascorbate is added 38 ms after previously reacting with *m*CPBA in the first mix, the ascorbate reacts to produce ferric heme (Fig. 6). Two phases are observed, one at ~160 s^{-1} and the other at ~12 s^{-1}, and we propose that they are largely due to the reduction of Cpd I and Cpd II (or unprotonated Cpd ES), respectively. Comparison of Fig. 6 (pH 8) and Fig. 7 (pH 7.4) shows that the ferric CYP153A6 is formed considerably faster at pH 8 than at pH 7.4. This could be due to greater access to ascorbate and/or greater reactivity at pH 8.

In our previous studies on P450cam we showed [15] that Cpd ES is formed when there is no suitable substrate present (and possibly when the substrate is incorrectly positioned for hydroxylation). Cpd ES can be reduced to Cpd II and then to ferric P450, thus uncoupling the reaction and yielding water as a product. In cells, the associated P450 reductase systems can carry this reduction of oxygen to water efficiently so that reactive oxygen species are not released to the solution. Previously, we showed that in P450 BM3 [19], Cpd ES is rapidly reduced to the ferric state by the physiological electron donor, NADPH, through the fused reductase domain. In our double mixing experiments described above, we showed that without reductase present ascorbate (and even NAD(P)H) could reduce Cpd ES to the ferric state. If substrate is present and correctly positioned, hydroxylation occurs, without formation of Cpd ES.

A model of CYP153A6 based on its homology with P450cam suggested to Funhoff et al. [32] that Ile103 of CYP153A6 (a residue that has no homology in P450cam) is essential for promoting hydroxylation at the terminal position of alkanes. Xu et al. showed that replacement of Tyr96 with Phe and Thr101 with Leu101 in P450cam changed the selectivity for substrates for hydroxylation from camphor to linear alkanes [48]. As was reported, the Thr101 mutation allows the camphor to slide towards the 101 side chain and reorient substrate for more efficient oxidation [49].

The appropriate orientation for ω-hydroxylation for CYP153A6 might occur during structural rearrangements in the reaction of heptane-bound CYP153A6 with *m*CPBA within the first 100 ms (Fig. 8, inset). These structural changes could mask the real rates for hydroxylation. However, we note that Cpd ES was not detected (Fig. 8), implying that the active hydroxylating species (probably Cpd I) attacks the properly positioned substrate before intramolecular electron transfer can occur. In general, product formation requires optimal distance and orientation of the substrate with respect to the ferryl intermediate. Our control using *m*-chlorobenzoic acid strongly suggested that the conversion to low spin ferric P450 was not simply a displacement of the heptane substrate.

These studies show that in contrast to camphor-bound P450cam, heptane-bound CYP153A6 has some access to oxidants (Fig. 8). Thus, CYP153A6 is a potential biocatalyst that can be

driven by peracids (or other artificial oxidants) with no added NAD(P)H or reductase in reactions using the shunt pathway for use in bioremediation and industrial applications. For example, CYP153A6 could be used as an alternative to the self-sufficient P450BM3 (that requires NADPH as a substrate) [50] for such purposes.

Acknowledgments

We acknowledge the Office of the Vice President for research and Department of Biochemistry of the University of Michigan for partial support of these studies. We are very grateful to Dr. J. Windak, Supervisor of Instrumental Service, Chemistry Department of the University of Michigan, for his assistance in setting up GC/MS analysis and his helpful comments.

Support for this work was provided by a grant from the National Institutes of Health, GM20877, to D.P.B.

References

1. Ortiz de Montellano, P. Cytochrome P450: Structure, Mechanism and Biochemistry. Plenum; NY: 1995.
2. Hayaishi, O. Molecular Mechanisms of Oxygen Activation. New York: 1974.
3. Groves JT. The bioinorganic chemistry of iron in oxygenases and supramolecular assemblies. Proc Natl Acad Sci U S A 2003;100:3569–3574. [PubMed: 12655056]
4. Coon MJ. Multiple oxidants and multiple mechanisms in cytochrome P450 catalysis. Biochem Biophys Res Commun 2003;312:163–168. [PubMed: 14630036]
5. Davydov R, Makris TM, Kofman V, Werst DE, Sligar SG, Hoffman BM. Hydroxylation of camphor by reduced oxy-cytochrome P450cam: Mechanistic implications of EPR and ENDOR studies of catalytic intermediates in native and mutant enzymes. J Am Chem Soc 2001;123:1403–1415. [PubMed: 11456714]
6. Sligar SG, Makris TM, Denisov IG. Thirty years of microbial P450 monooxygenase research: peroxo-heme intermediates--the central bus station in heme oxygenase catalysis. Biochem Biophys Res Commun 2005;338:346–354. [PubMed: 16139790]
7. Newcomb M, Chandrasena RE. Highly reactive electrophilic oxidants in cytochrome P450 catalysis. Biochem Biophys Res Commun 2005;338:394–403. [PubMed: 16168951]
8. Nam W, Ryu YO, Song WJ. Oxidizing intermediates in cytochrome P450 model reactions. J Biol Inorg Chem 2004;9:654–660. [PubMed: 15365902]
9. McLain, J.; Lee, J.; Groves, JT. Biomimetic Oxydations Related to Cytochrome P450: Metal-Oxo and Metal-Peroxo Intermediates. In: Meunier, B., editor. Biomimetic Oxidations Catalyzed by Transition Metal Complexes. Imperial College Press; London: 2000. p. 91-170.
10. Egawa T, Shimada H, Ishimura Y. Evidence for compound I formation in the reaction of cytochrome P450cam with m-chloroperbenzoic acid. Biochem Biophys Res Commun 1994;201:1464–1469. [PubMed: 8024592]
11. Kellner DG, Hung SC, Weiss KE, Sligar SG. Kinetic characterization of Compound I formation in the thermostable cytochrome P450 CYP119. J Biol Chem 2002;277:9641–9644. [PubMed: 11799104]
12. Sono M, Roach MP, Coulter ED, Dawson JH. Heme-Containing Oxygenases. Chem Rev 1996;96:2841–2887. [PubMed: 11848843]
13. Issak, IS.; Dawson, JH. Haem Iron-Containing Peroxidases. In: Ballou, DP., editor. Essays in Biochemistry. Portland Press; Princenton, NJ: 1999. p. 51-69.
14. Spolitak T, Dawson JH, Ballou DP. Reaction of ferric cytochrome P450cam with peracids: kinetic characterization of intermediates on the reaction pathway. J Biol Chem 2005;280:20300–20309. [PubMed: 15781454]
15. Spolitak T, Dawson JH, Ballou DP. Rapid kinetics investigations of peracid oxidation of ferric cytochrome P450cam: nature and possible function of compound ES. J Inorg Biochem 2006;100:2034–2044. [PubMed: 17095096]
16. Schünemann V, Lendzian F, Jung C, Contzen J, Barra AL, Sligar SG, Trautwein AX. Tyrosine radical formation in the reaction of wild type and mutant cytochrome P450cam with peroxy acids: a

multifrequency EPR study of intermediates on the millisecond time scale. J Biol Chem 2004;279:10919–10930. [PubMed: 14688245]

17. Schünemann V, Jung C, Terner J, Trautwein AX, Weiss R. Spectroscopic studies of peroxyacetic acid reaction intermediates of cytochrome P450cam and chloroperoxidase. J Inorg Biochem 2002;91:586–596. [PubMed: 12237224]
18. Jung C, Schunemann V, Lendzian F. Freeze-quenched iron-oxo intermediates in cytochromes P450. Biochem Biophys Res Commun 2005;338:355–364. [PubMed: 16143295]
19. Raner GM, Thompson JI, Haddy A, Tangham V, Bynum N, Ramachandra Reddy G, Ballou DP, Dawson JH. Spectroscopic investigations of intermediates in the reaction of cytochrome P450(BM3)-F87G with surrogate oxygen atom donors. J Inorg Biochem 2006;100:2045–2053. [PubMed: 17083977]
20. Spolitak T, Dawson JH, Ballou DP. Replacement of tyrosine residues by phenylalanine in cytochrome P450cam alters the formation of Cpd II-like species in reactions with artificial oxidants. J Biol Inorg Chem 2008;13:599–611. [PubMed: 18273651]
21. Hessenauer-Ilicheva N, Franke A, Meyer D, Woggon WD, van Eldik R. Mechanistic Insight into Formation of Oxo-Iron(IV) Porphyrin pi-Cation Radicals from Enzyme Mimics of Cytochrome P450 in Organic Solvents. Chemistry- Eur J 2009;15:2941–2959.
22. Khavrutskii IV, Musaev DG, Morokuma K. Cooperative pull and push effects on the O-O bond cleavage in acylperoxo complexes of [(Salen)(MnL)-L-III]: Ensuring formation of manganese(V) oxo species. Inorg Chem 2005;44:306–315. [PubMed: 15651877]
23. Yamaguchi K, Watanabe Y, Morishima I. Direct Observation of Push Effect on the Heterolytic O-O Bond-Cleavage Reaction of Acylperoxo-Iron(III) Porphyrin Adducts. Journal of the Chemical Society-Chem Commun 1992:1709–1710.
24. Machii K, Watanabe Y, Morishima I. Acylperoxo-Iron(III) Porphyrin Complexes - a New Entry of Potent Oxidants for the Alkene Epoxidation. J Am Chem Soc 1995;117:6691–6697.
25. Matsui T, Nagano S, Ishimori K, Watanabe Y, Morishima I. Preparation and reactions of myoglobin mutants bearing both proximal cysteine ligand and hydrophobic distal cavity: protein models for the active site of P-450. Biochemistry 1996;35:13118–13124. [PubMed: 8855949]
26. Wiseman B, Colin J, Smith AT, Ivancich A, Loewen PC. Mechanistic insight into the initiation step of the reaction of Burkholderia pseudomallei catalase-peroxidase with peroxyacetic acid. J Biol Inorg Chem 2009;14:801–811. [PubMed: 19290552]
27. Ichikawa Y, Nakajima H, Watanabe Y. Characterization of peroxide-bound heme species generated in the reaction of thermally tolerant cytochrome c552 with hydrogen peroxide. Chembiochem 2006;7:1582–1589. [PubMed: 16921577]
28. Brittain T, Baker AR, Butler CS, Little RH, Lowe DJ, Greenwood C, Watmough NJ. Reaction of variant sperm-whale myoglobins with hydrogen peroxide: the effects of mutating a histidine residue in the haem distal pocket. Biochem J 1997;326:109–115. [PubMed: 9337857]
29. Green AJ, Rivers SL, Cheeseman M, Reid GA, Quaroni LG, Macdonald ID, Chapman SK, Munro AW. Expression, purification and characterization of cytochrome P450 Biol: a novel P450 involved in biotin synthesis in Bacillus subtilis. J Biol Inorg Chem 2001;6:523–533. [PubMed: 11472016]
30. Hawkes DB, Adams GW, Burlingame AL, Ortiz de Montellano PR, De Voss JJ. Cytochrome P450 (cin) (CYP176A), isolation, expression, and characterization. J Biol Chem 2002;277:27725–27732. [PubMed: 12016226]
31. McLean MA, Maves SA, Weiss KE, Krepich S, Sligar SG. Characterization of a cytochrome P450 from the acidothermophilic archaea Sulfolobus solfataricus. Biochem Biophys Res Commun 1998;252:166–172. [PubMed: 9813164]
32. Funhoff EG, Bauer U, Garcia-Rubio I, Witholt B, van Beilen JB. CYP153A6, a soluble P450 oxygenase catalyzing terminal-alkane hydroxylation. J Bacteriol 2006;188:5220–5227. [PubMed: 16816194]
33. Asperger O, Naumann A, Lkeber HP. FEMS Microbiol. Lett 1981;11:309–312.
34. Eremina SS, Asperger O, Kleber HP. Cytochrome P-450 and the respiratory activity of Acinetobacter calcoaceticus growing on n-nonane. Mikrobiologiia 1987;56:764–769. [PubMed: 3448466]
35. van Beilen JB, Funhoff EG, van Loon A, Just A, Kaysser L, Bouza M, Holtackers R, Rothlisberger M, Li Z, Witholt B. Cytochrome P450 alkane hydroxylases of the CYP153 family are common in

alkane-degrading eubacteria lacking integral membrane alkane hydroxylases. Appl Environ Microbiol 2006;72:59–65. [PubMed: 16391025]

36. Li Z, Chang DL. Recent advances in regio- and stereoselective biohydroxylation of non-activated carbon atoms. Current Organic Chemistry 2004;8:1647–1658.
37. van Beilen JB, Holtackers R, Luscher D, Bauer U, Witholt B, Duetz WA. Biocatalytic production of perillyl alcohol from limonene by using a novel Mycobacterium sp cytochrome P450 alkane hydroxylase expressed in Pseudomonas putida. Appl Environl Microbiol 2005;71:1737–1744.
38. Urlacher VB, Schmid RD. Recent advances in oxygenase-catalyzed biotransformations. Curr Opin Chem Biol 2006;10:156–161. [PubMed: 16488653]
39. Cotton ML, D HB, R JM. Studies on Horseradish Peroxidase. 13. The Kinetic Effect of Cyanide on the Oxidation-Reduction Cycle. Can J Biochem 1973;51(5):627–631. [PubMed: 4706838]
40. Bevington, PR. Data Reduction and Error Analysis for the Physical Sciences. McGraw-Hill Inc; New York: 1996. p. 235-242.
41. Palcic MM, Rutter R, Araiso T, Hager LP, Dunford HB. Spectrum of Chloroperoxidase Compound I. Biochem Biophys Res Commun 1980;94:1123–1127. [PubMed: 7190391]
42. Rutter R, Hager LP, Dhonau H, Hendrich M, Valentine M, Debrunner P. Chloroperoxidase compound I: Electron paramagnetic resonance and Mossbauer studies. Biochemistry 1984;23:6809–6816. [PubMed: 6099143]
43. Schunemann V, Jung C, Trautwein AX, Mandon D, Weiss R. Intermediates in the reaction of substrate-free cytochrome P450cam with peroxy acetic acid. FEBS Lett 2000;479:149–154. [PubMed: 10981725]
44. Prasad S, Mazumdar S, Mitra S. Binding of camphor to Pseudomonas putida cytochrome p450(cam): steady-state and picosecond time-resolved fluorescence studies. FEBS Lett 2000;477:157–160. [PubMed: 10908713]
45. Griffin BW, Peterson JA. Camphor binding by Pseudomonas putida cytochrome P-450. Kinetics and thermodynamics of the reaction. Biochemistry 1972;11:4740–4746. [PubMed: 4655251]
46. Atkins WM, Sligar SG. The roles of active site hydrogen bonding in cytochrome P-450cam as revealed by site-directed mutagenesis. J Biol Chem 1988;263:18842–18849. [PubMed: 3198602]
47. Matsui T, Ozaki S, Watanabe Y. Formation and catalytic roles of compound I in the hydrogen peroxide-dependent oxidations by His64 myoglobin mutants. J Am Chem Soc 1999;121:9952–9957.
48. Xu F, Bell SG, Lednik J, Insley A, Rao Z, Wong LL. The heme monooxygenase cytochrome P450cam can be engineered to oxidize ethane to ethanol. Angew Chem Int Ed Engl 2005;44:4029–4032. [PubMed: 15912546]
49. Xu F, Bell SG, Rao Z, Wong LL. Structure-activity correlations in pentachlorobenzene oxidation by engineered cytochrome P450cam. Protein Eng Des Sel 2007;20:473–480. [PubMed: 17962225]
50. Munro AW, Girvan HM, McLean KJ. Cytochrome P450-redox partner fusion enzymes. Biochim Biophys Acta 2007;1770:345–359. [PubMed: 17023115]

ABBREVIATIONS

P450	cytochrome P450
CYP153A6	CYP153A6 from *Mycobacterium* sp. HXN-1500
P450cam	cytochrome P450cam isolated from *Pseudomonas putida*
Cpd I	state of cytochrome P450 or peroxidase that is 2 equivalents of oxidation greater than the ferric form and contains an oxoferryl center (Fe^{IV}=O) and a porphyrin π-cation radical
Cpd II	state of cytochrome P450 or peroxidase that contains an oxoferryl center (Fe^{IV}=O) and is one equivalent of oxidation greater than the ferric form
CPO	chloroperoxidase from *Caldariomyces fumago*
HRP	horseradish peroxidase

CcP	cytochrome *c* peroxidase
Cpd ES	the 2-electron-oxidized state of P450 or peroxidases containing both an oxoferryl center (Fe^{IV}=O) and either a tryptophanyl or tyrosyl radical, analogous to Cpd ES in CcP
*m*CPBA	*meta*-chloroperbenzoic acid
PAA	peracetic acid
TMPD	N,N,N,N-tetramethyl-*p*-phenylenediamine
ABTS	2,2’-azinobis (3-ethylbenzthiazoline-6-sulfonate
DMSO	methyl sulfoxide
RFQ-EPR	rapid freeze-quench electron paramagnetic resonance spectroscopy

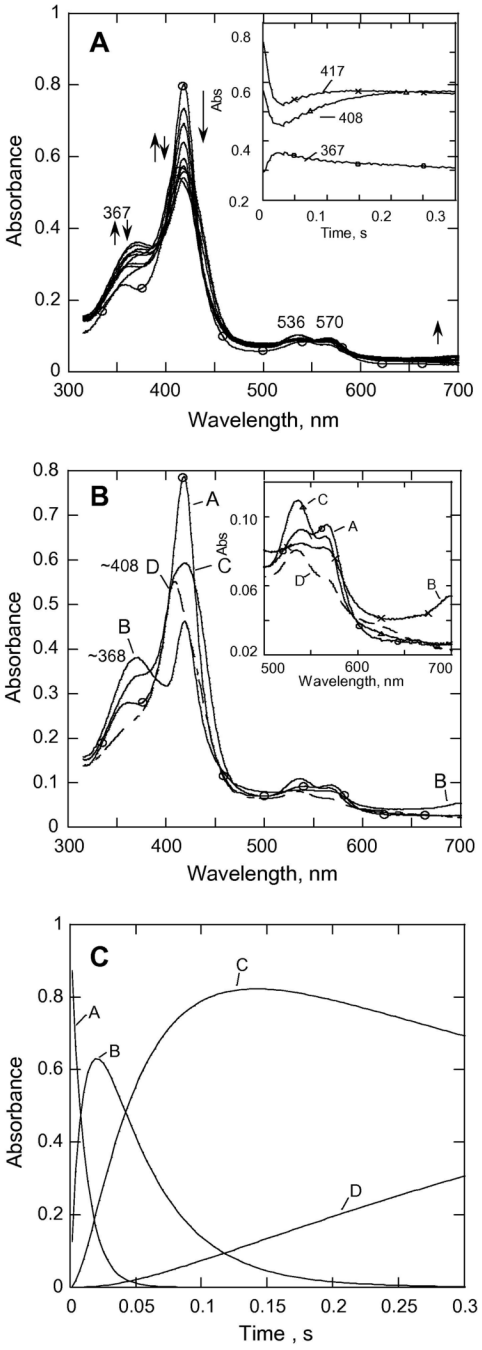

Fig. 1.

(A) Rapid-scan absorbance data for the reaction of CYP153A6 with *m*CPBA at 25 °C, pH = 8.0, P450, 7.1 μM; *m*CPBA, 150 μM. Selected spectra from 0 to 0.3 s are shown. Inset, data recorded at indicated wavelengths. (B) SVD analysis of the rapid scan data recorded for the reaction in (A). Model used was A→B→C→D with k_1 = 91 s^{-1}, k_2 = 22. 5 s^{-1}, k_3 = 1.5 s^{-1}. A (–○–○–); B (– – –); C (–x–x–); D (--Δ--Δ-).

Inset, expansion of data in the visible region. (C) Molar fractions of the different forms of CYP153A6 on the reaction pathway from (B).

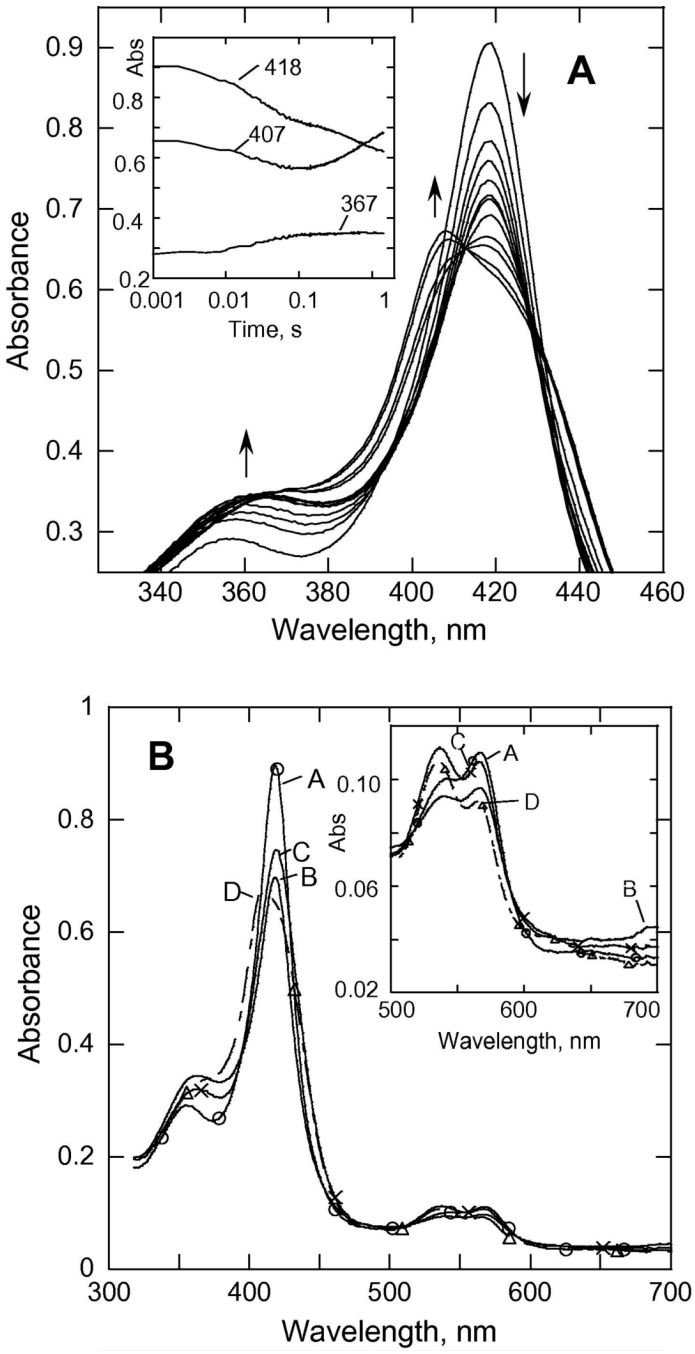

Fig. 2.

(A). Rapid-scan absorbance data for the reaction of CYP153A6 (7.2 μM) with *m*CPBA at pH8.0, 3.4 °C. To show spectral changes more clearly, the peak of the Soret band has been expanded. Inset, data recorded at indicated wavelengths. (B) SVD analysis of the rapid scan recorded for the reaction in (A). Model used was A→B→C→D with k_1 = 34 s^{-1}, k_2 = 3 s^{-1}, k_3 = 1.4 s^{-1}. A (–○–○–); (– – –); C (–x–x–); D (--Δ--Δ-).

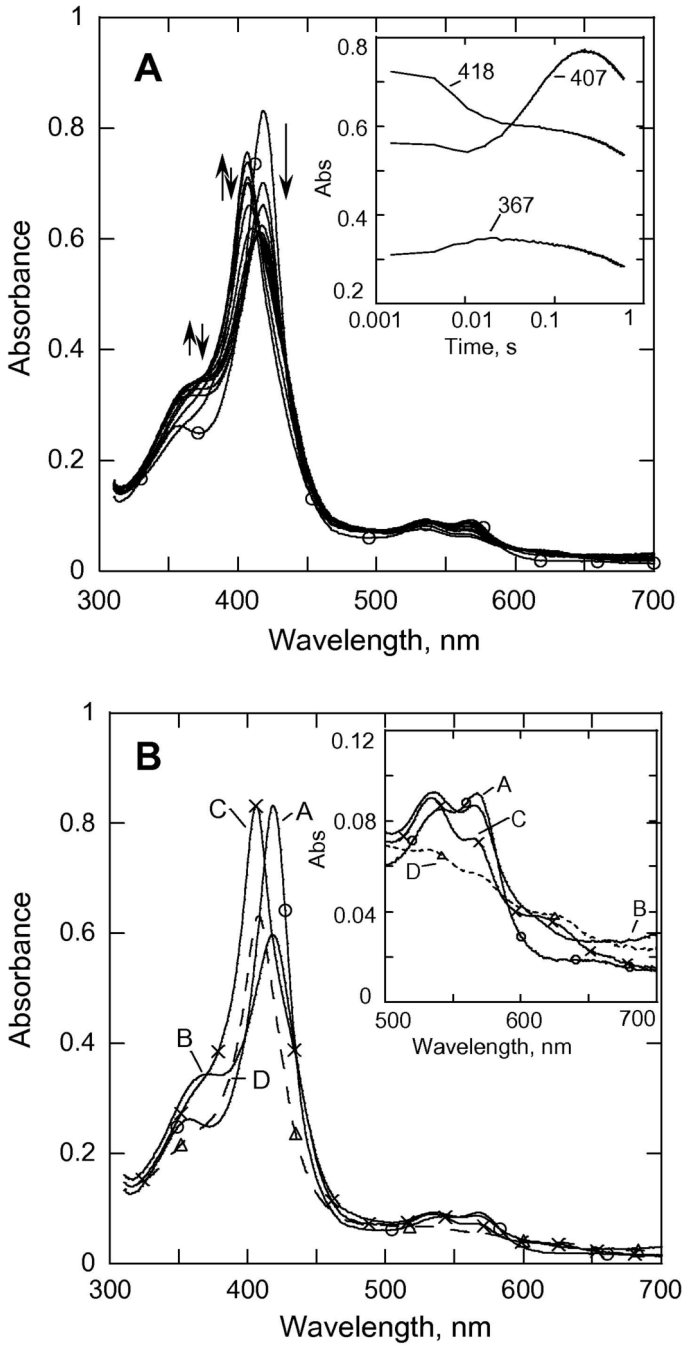

Fig. 3.

(A). Rapid-scan absorbance data for the reaction of CYP153A6 (~7.1 μM) with *m*CPBA (150 μM) from 0 to 0.6 s at pH = 7.4, 25.0 °C. Inset, data recorded at selected wavelengths. (B) SVD analysis of the rapid scan recorded for the reaction in (A). Model used was A→B→C→D with k_1 = 120 s^{-1}, k_2 = 13.5 s^{-1}, k_3 = 1.9 s^{-1}. A (–○–○–); B (– – –); C (–x–x–); D (--Δ--Δ-).

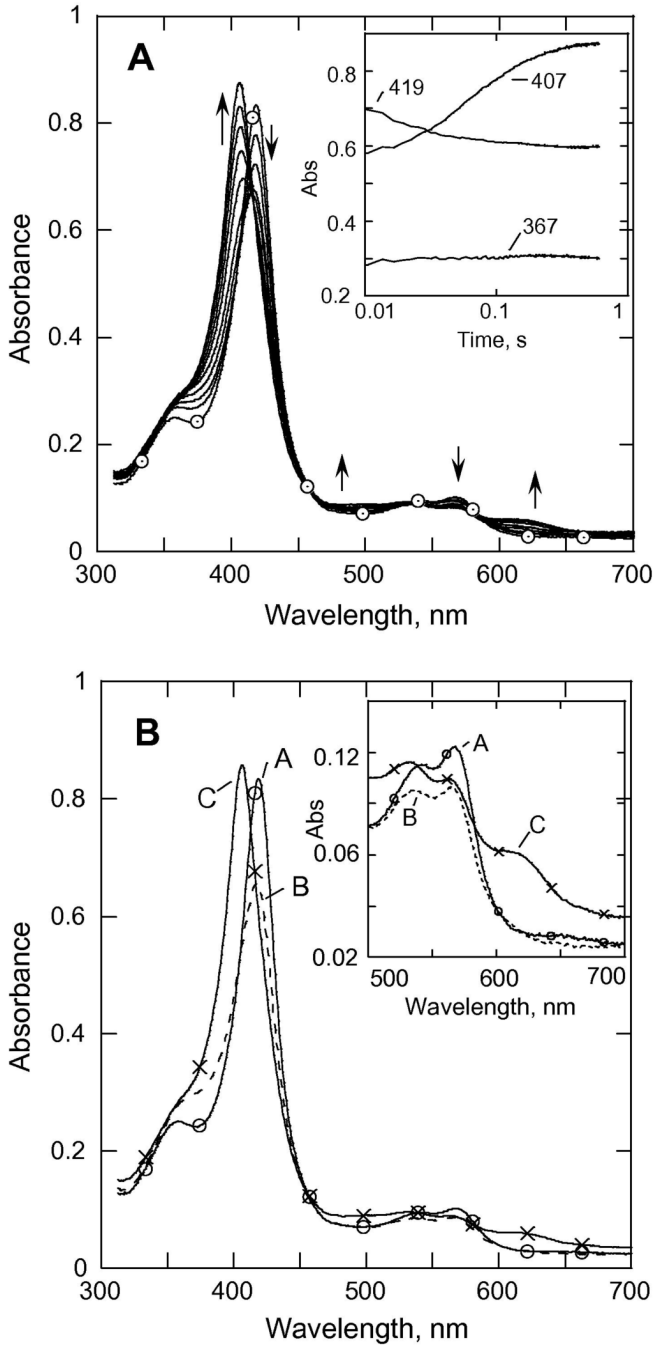

Fig. 4.

(A). Rapid-scan absorbance data for the reaction of CYP153A6 (~7.2 μM) with *m*CPBA (38 μM) from 0 to 0.6 s at pH 6.2; 25.0 °C. Inset, data recorded at selected wavelengths. (B) SVD analysis of the rapid scan recorded for the reaction in (A). Model used was A→B→C→D with k_1 = 85 s^{-1}, k_2 = 12.5 s^{-1}, A (–○–○–); B (– – –); C (–x–x–)

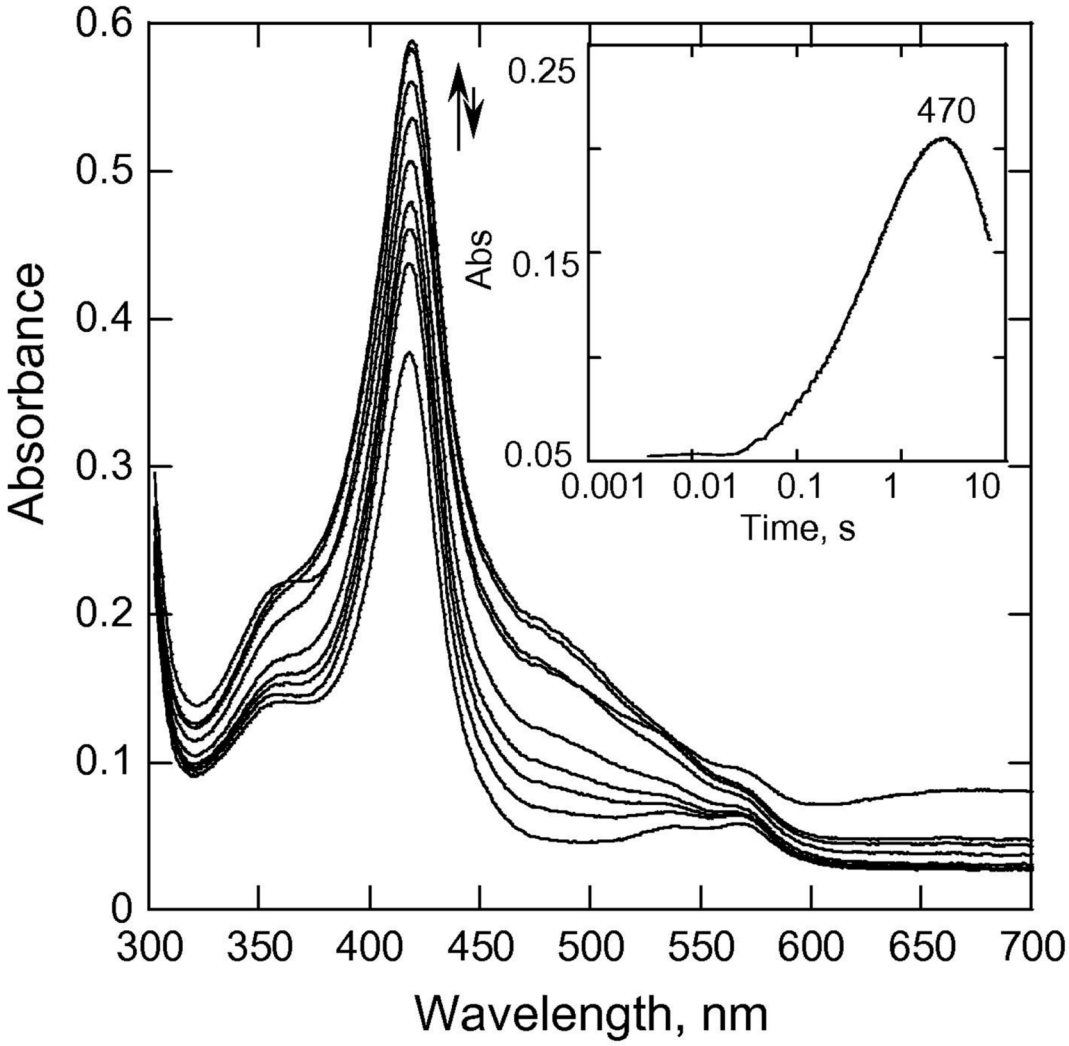

Fig. 5.

Rapid-scan absorbance data for the reaction of CYP153A6 (~15.5 μM –initial concentration) in double mixing experiments with *m*CPBA (300 μM, I mix) and introducing guaiacol (9.6 mM) in the second mix (age time 36 ms) from 0 to 7.44 s at pH 8.0, 25.0 °C. Inset, data recorded at selected wavelength.

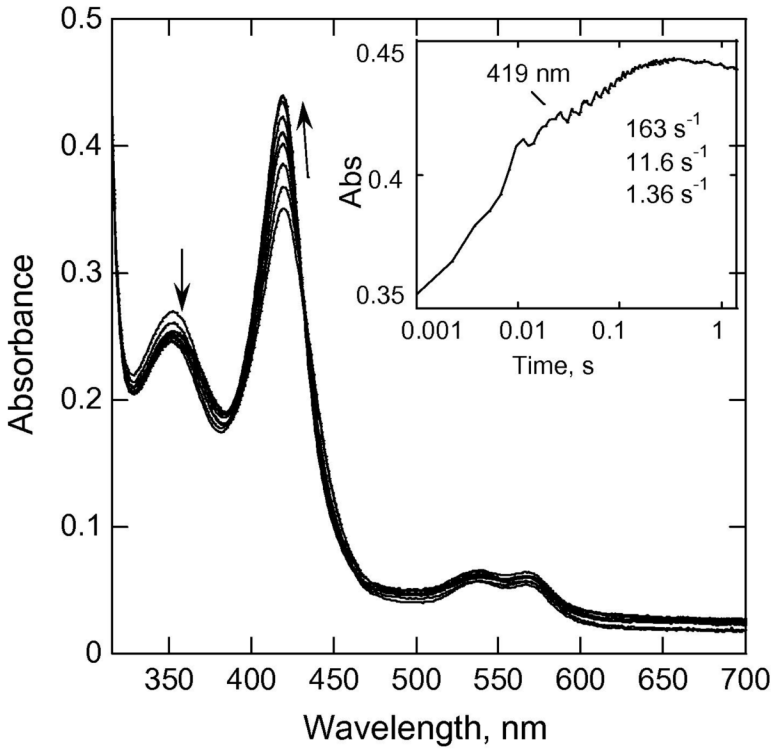

Fig. 6.

Double mixing experiments showing spectral changes upon mixing CYP153A6 (~15.8 μM before mixing) with *m*CPBA (300 μM *m*CPBA before mixing) at pH 8.0, 25 C in the first mix, and ascorbic acid (20 mM final concentration) in the second mix (age time 38.5 ms). Note that a species with a Soret band at ~421 nm is formed, and it converts back to ferric (Soret peak at ~418 nm). Inset, absorbance trace at selected wavelength.

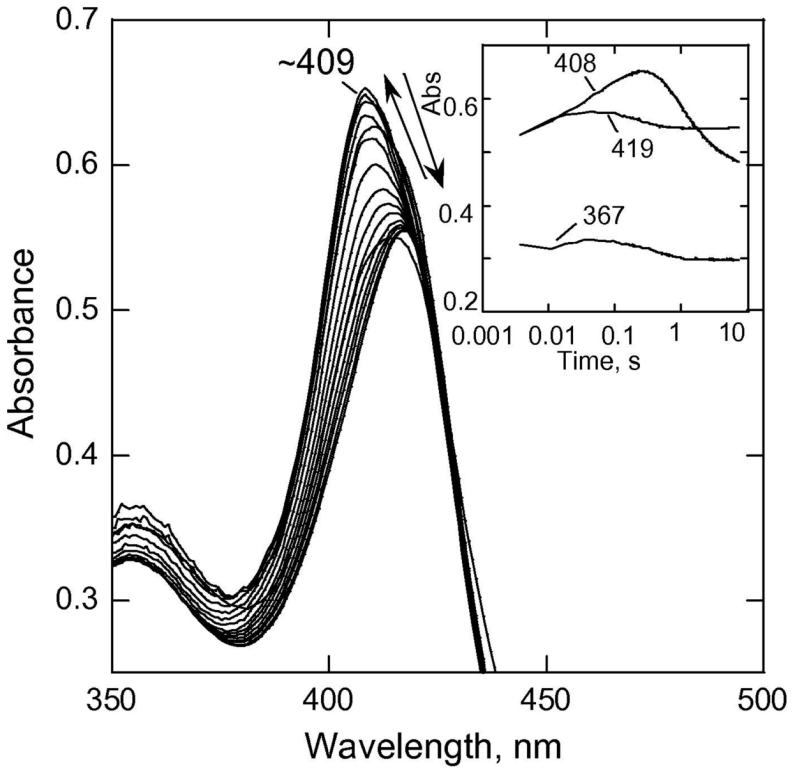

Fig. 7.

Double mixing experiments showing spectral changes upon mixing CYP153A6 (~28.8 μM before mixing) with *m*CPBA (600 μM *m*CPBA before mixing) at pH 7.4, 25 °C in the first mix, and ascorbic acid (20 mM final concentration) in the second mix (age time 55.4 ms). To show spectral changes more clearly, the peak of the Soret band has been expanded. Inset, absorbance traces at selected wavelengths.

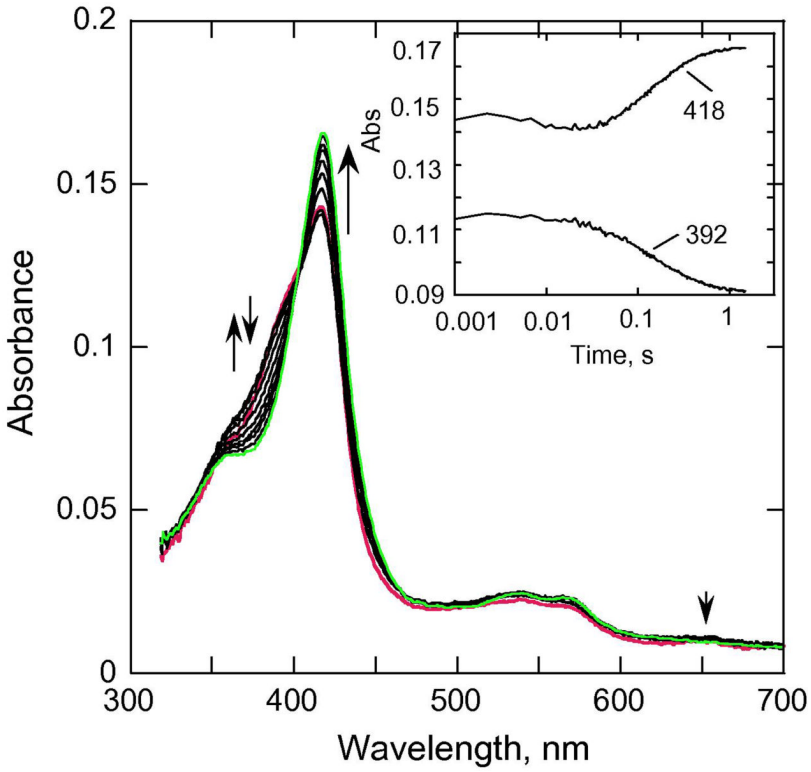

Fig. 8.

Double mixing experiments showing spectral changes upon mixing CYP153A6 (~6 μM before mixing) with heptane (500 μM before mixing) at pH 7.4, 25 °C in the first mix, aged for 100 s, and then mixed with *m*CPBA (300 μM initial concentration) in the second mix. Inset, absorbance traces at selected wavelengths.